9

Imaging Living Chondrocyte Surface Structures With AFM Contact Mode

Gerlinde Bischoff, Anke Bernstein, David Wohlrab, and Hans-Joachim Hein

1. Introduction

In its most established mode of operation, named constant force contact mode, atomic force microscopy (AFM) has been applied to image the 2D and 3D architecture of surfaces. Any deflection of the tip as a result of surface topography is recorded. The microscope reconstructs an image of the surface from the *x*, *y*, and *z* scan data to develop a 3D illustration of any surface at the micro- and nanometer level. The production of high-resolution images of a wide variety of biological samples at near-native conditions and the possibility to measure very low local forces is proving to be a powerful tool for cell analysis ***(1,2)***. In contrast with electron microscopy observations in particular, AFM improves biological studies involving imaging by also monitoring dynamic processes. However, the investigation of soft biomaterials with this special method is still challenging. This chapter reviews practical details of imaging two cell lines: human chondrocytes and human osteosarcoma. However, characteristics described are not unique to this type of cell. Principally, all types of adherently growing cells can be investigated with the techniques described here. Force curve analysis, as a backdrop for the understanding of the received images ***(1)***, will be introduced in detail in **Subheading 3.4.** Further sections explore how AFM can be used as a helpful tool in observations of the cell surface and the physical interactions that occur there, like adhesion or friction, and their influence on the active cell. In **Subheading 7.** common artifacts and troubles are described, along with the practical instructions.

From: *Methods in Molecular Biology, vol. 242: Atomic Force Microscopy: Biomedical Methods and Applications*
Edited by: P. C. Braga and D. Ricci © Humana Press Inc., Totowa, NJ

2. Cell Lines

2.1. Characteristics of Chondrocytes

Investigations were performed on human chondrocytes isolated from human osteoarthritic knee joint cartilage. The cartilage was isolated from cartilage bone fragments resected during the insertion of knee prostheses. All patients presented gonarthritis. No other relevant disease—particularly rheumatoid arthritis—was present. Immediately after the resection, the cartilage bone-fragments were potted in sterile L15 medium (Seromed, Berlin, Germany). Thereafter, the cartilage was handled as described elsewhere ***(3)***.

Cartilage is comprised of a large amount of functional extracellular matrix that is made and maintained by a small number of chondrocytes, the sole resident cell type. Chondroblasts and chondrocytes secrete cartilage matrix, and chondrocytes are also embedded therein. The bones of a developing or restoring limb form through the process of endochondral bone formation. In the beginning, mesenchymal cells condense and cells in the core differentiate into chondrocytes, and the cells at the periphery differentiate into the perichondrium. Articular cartilage has several features that impact on the fate of bioactive bodies. Chondrocytes are anchored in the extracellular matrix and are surrounded by a pericellular matrix. Of particular interest regarding dense connective tissues, recent experiments have shown that mechanotransduction is critically important in vivo in the cell-mediated feedback among physical stimuli, the molecular structure of matrix molecules (e.g., collagen), and the resulting macroscopic biomechanical properties of the tissue ***(4–7)***.

2.2. Characteristics of Human Osteosarcoma

Human osteosarcoma (HOS), a human osteogenic sarcoma cell line, was purchased from American Type Culture Collection (Rockville, MD). The cells were cultured in a medium volume equivalent to 1:1 mixture of Dulbecco's modified Eagle's medium (DMEM) and Ham's F-12 medium containing penicillin (100 U/mL) and streptomycin (100 µg/mL) and 10 vol% fetal bovine serum. The HOS cells exhibit a flat morphology, low saturation density, low plating efficiency in soft agar, and are sensitive to chemical and viral transformation ***(4)***.

The nontumorigenic, as well as the immortal tumorigenic, osteoblast-like human osteosarcoma cells are used in many laboratories along with their large number of derivatives. Because they are one type of potential hormone-related cancer, the number of studies is incredibly high ***(8,9)***. For these cells to reach their functional differentiated state the action of specific factors is required.

Mechanical stress is an important regulator of bone metabolism. Fluid shear stress caused by mechanical load in bone tissue has been shown to be impor-

tant to both the bone structure and function through its effects on osteocytes and osteoblasts. Many hypotheses about the mechanotransduction system in bone cells have been proposed. Recent findings suggest that the physiological level of fluid shear stress induces the production of crucial proteins in human osteosarcoma cells via the cation channel function and, as a result, may therefore promote bone formation ***(10)***.

3. AFM Contact Mode in Biology

In an AFM the tip is mounted on the end of a flexible cantilever. As the sample is scanned beneath the tip, small forces of interaction with the sample cause the cantilever to deflect, revealing the sample's topography. The most common approach—called an optical lever—is to reflect a laser beam off the backside (upper side) of the cantilever into a four-segment photodetector (quadrant). The difference in output between the detectors is then proportional to the deflection amplitude. Important to note is that the limiting factor in motion detectors is not the sensitivity of the photodetector itself (deflections as small as 0.01 nm can be detected), but the intrinsic vibration of the cantilever attributable to Brownian motion.

The cantilever is integrated with a sharp tip on the end and characterized by its material (usually silicon nitride for contact mode investigations), its spring constant, and its geometric properties (usually parabolic or pyramidal tip shape with a curvature radius of 20–40 nm). The spring constant, k_n (determined by thermal vibration in air) varies from 0.06–5 N/m. Low spring constants are sensitive to uncontrolled vibration of the tip released by tip–sample interactions.

3.1. Contact Mode Description

In the contact mode, the tip touches the surfaces at all times with constant force, sliding over the surface as the sample is scanned line by line. Thereby topographic information is received by monitoring the change in cantilever deflection. Force-distance curves are obtained by plotting the vertical displacement of the cantilever, as a function of the separation between the tip and the sample. The force curve is an approach-retract cycle, in which the sample first approaches the tip (*see* **Fig. 1**) and is subsequently retracted from the tip. The cantilever deflection Δz is then converted into force (F_n) according to the relationship ***(11)***:

$$F_n = k_N \Delta z$$

Since normal spring constants for cantilevers are 0.01–100 N/m and instrumental sensitivities for normal deflections are up to approx 0.01 nm, the corresponding limits in force detection are 10^{-13}–10^{-8} *N* ***(12)***.

Because of their softness, the biological membranes of viable cells become significantly indented upon contact by the AFM scanning tip, even at low

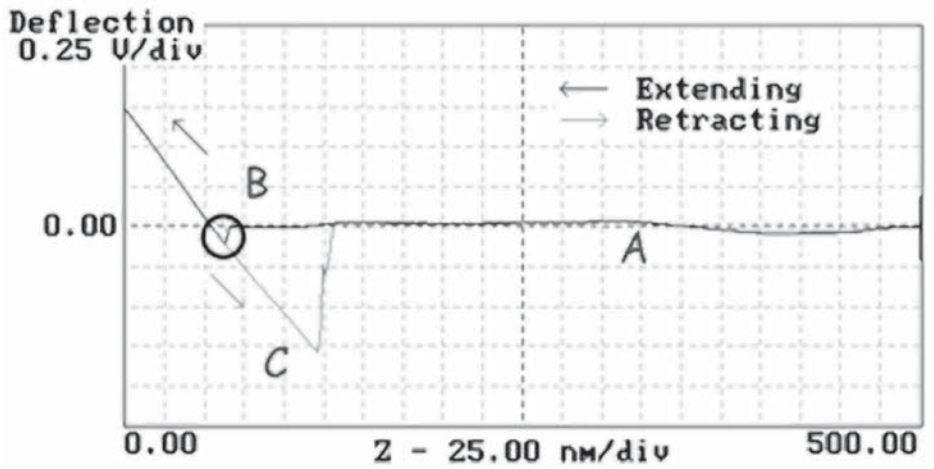

Fig. 1. Favorable force–distance curve of an adherent cell. **(A)** No interaction force detectable at large tip–sample distances. The distance of the scanner movement is represented by the horizontal axis, and the cantilever deflection is represented by the vertical axis. In the case shown, there are minimal long-range forces, so this "noncontact" part of the force curve shows no deflection. **(B)** As the probe tip is brought very close to the surface, it may jump into contact (see circled area), if it feels sufficient attractive force from the sample. Sometimes repulsion force induces elongation in other directions. As the tip moves further in the positive *z* direction, a positive linear cantilever deflection is observed as the tip and sample move together. If the cantilever is sufficiently stiff, the probe tip is able to indent into the surface at this point. If this takes place, the slope of the contact part of the force curve can provide information about the elasticity of the sample surface ***(12)***. After loading the cantilever to a desired force value, the process is reversed. As the sample moves in the opposite (negative) *z* direction, a similar cantilever deflection line is traced as the tip and sample remain in contact. **(C)** As the tip moves further in the negative *z* direction, the restoring force exerted by the bending of the cantilever overcomes the adhesive force of the tip–sample contact. At this point, the adhesion is broken and the cantilever comes free from the surface. This can be used to measure the rupture force required to break the bond or adhesion ***(12,13)***.

forces. Always exercise caution when interpreting the topographic features, however, because of the convolution of the tip shape ***(1,11–14)***.

To this point, we have focused on imaging mechanisms that rely on deflections of the tip with respect to the surface normal. The force generated when the tip is moved laterally over the sample surface can also be used as an imaging mechanism (phase or friction mode). The energy differences in trace-retrace plots are indicative of the energy dissipated in the scan. Attractive and repul-

sive forces lead to information about the hydrophobicity and hydrophilicity of the specimen ***(15)***. Changes in the "friction" images indicate quite well the tip–surface interactions. This is also true of a tip with a truncated apex ratio—the lateral force is rather insensitive to minor cantilever stiffness, different from the topography scan ***(16,17)***. In the case of round massive cells, high lateral forces, however, still hamper stable imaging (*see* Chapter 4).

4. AFM Instrumentations

AFM investigations were done at room temperature in air (samples covered with a droplet of water) or in buffer solution. We used the commercially available Digital Instruments Nanoscope III in constant force contact mode. Generally, the 512×512 pixel images were captured with a square scan-size between 0.6 and 100 µm at a scan rate of 0.2–5 scan lines/second (s) (0.2–5 Hz). Sharp Si_3N_4-cantilevers, each with a pyramidal tip, were used. Their spring constant was 0.1–5 N/m. Best results were obtained by using cantilevers with a spring constant about 0.5–1 N/m. To avoid cell damage, the feedback set point was adjusted frequently to 0.1–10 nN in order to optimize the contact force.

5. AFM Imaging Conditions

The data were acquired simultaneously with the height, the deflection, and the friction signals (*see* **Fig. 2** to distinguish between the modes). The height mode monitors the topography. The deflection mode, as the first derivation of the height mode, offers supplementary details of the cell structure. The friction signal was used to investigate the lateral force interaction between the tip and the sample.

AFM Si_3N_4 tips should in principle be oxidized and hydrophilic; however, in practice they will be hydrophobic owing to hydrocarbon contamination ***(11,12)***. Fluid imaging with AFM requires a special tip holder ("contact mode fluid cell" from VEECO Metrology Group [Mannheim, Germany] was used). For the microscopical studies, the chondrocytes and HOS cells were seeded onto round glass cover slips (4-mm diameter). These cover slips were attached to the bottom of the fluid cell with vacuum grease to standard magnetic AFM mounting plates, before being covered with some droplets of media. When the tip dives into the liquid medium, the laser reflections have to be carefully inspected to exclude "false" reflections, which occur when the tip comes in contact with the liquid surface. Usually our measurements were done at room temperature in aqueous phosphate buffer solution. Good imaging and detection of cell activity could be obtained in the constant force contact mode. The cantilever was carefully approached to the surface (*see* **Subheading 7.8.**), in order to collect the first images in the "low-contact" mode (**Fig. 1**, region B) and to avoid strong physical contact between the tip and the sample surface.

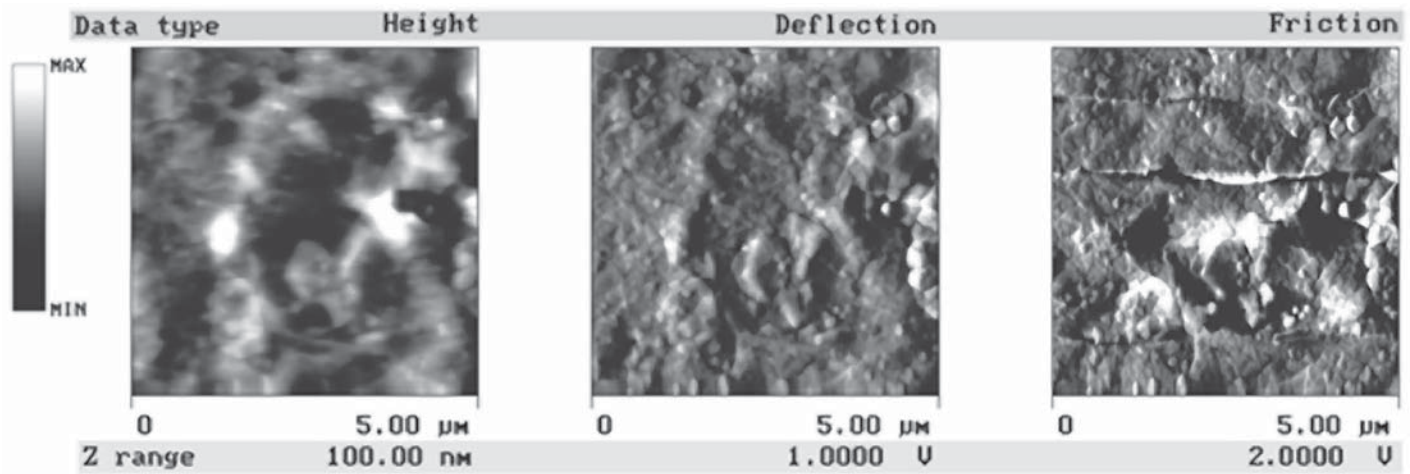

Fig. 2. Simultaneous AFM images of HOS cells in buffer observed with different modes: height (left), deflection (center), and friction (right). The topography is monitored by the height mode. The deflection mode, as the first derivation of the height mode, offers more details of the cell structure. The friction signal was used to investigate the lateral force interaction between the tip and the sample. Generally, large contrast in friction image often indicates active parts.

Later on, scans were done in contact mode with increased forces. Under favorable conditions, cells could be observed for up to 8 hours (h) depending on the cell viability ***(18)***. Frequently, undefinable cantilever vibrations induced by diffusion processes or cell motion are challenging problems. As a practical note, best observation conditions occur at night, when the neighborhood vibrations are minimized.

6. AFM Contact Mode Imaging of Living Cells

Cantilevers with a spring constant have a reduced sensitivity to vibrations and are used successfully to surmount undefinable cantilever deflection. It is of great importance to adjust and minimize the force carefully and to avoid cell damage (*see* **Subheading 7.**). In contact mode, true molecular resolutions could be achieved. The investigation of adherently growing cells with very low pressure on the tip resulted in diminished cell motion and improved the study. Well-resolved topographic information could be obtained. Zooming-in allows the recording of pictures with increasing detail. Especially in fluid medium, the investigation of active cells offers numerous facts. As an example of dynamic interactions, a series of images collected from chondrocytes and HOS cells in buffer is presented in **Figs. 3–6**).

High-resolution images of inner pore processes from the chondrocytes could be visualized (**Fig. 3** and **4**). During the pore diameter reduction, the surface potential in the immediate vicinity changes noticeably. The dynamic interaction is followed by secretion. Large differences (high contrast) in the friction images of several chondrocyte measurements (**Fig. 4**) point out an active part of the cell surface. The data was recorded during an interval of more than 2 h. The friction images remained a rather constant dynamic during this time ***(19)***. This is an indication of the viability of the material ***(18)***. This time interval of several hours seems long enough to study cell stimulations with mediators (e.g. cytokines, mitogens, enzyme substrates) and thus offers great promise for future experiments.

However, the round massive chondrocytes should not be as suitable for AFM observations as the flat HOS cells. In **(Fig. 5)**. the secretion on their cell surface is monitored (see in particular some cell excrements marked out in frames **A** and **B**). In this case, we were able to obtain good-quality images quite easily and visualize the cell structure. A collection of force-distance curves could be collected in order to control whether the tip indented the soft cell surface or not. Indentation increases with the applied force and reaches a maximum value, after which tip-soiling damage occurs. However, the surface penetration results in almost any case in more or less tip contamination. While the shape of the biofouled tip had broadened at the apex in comparison with that of the original

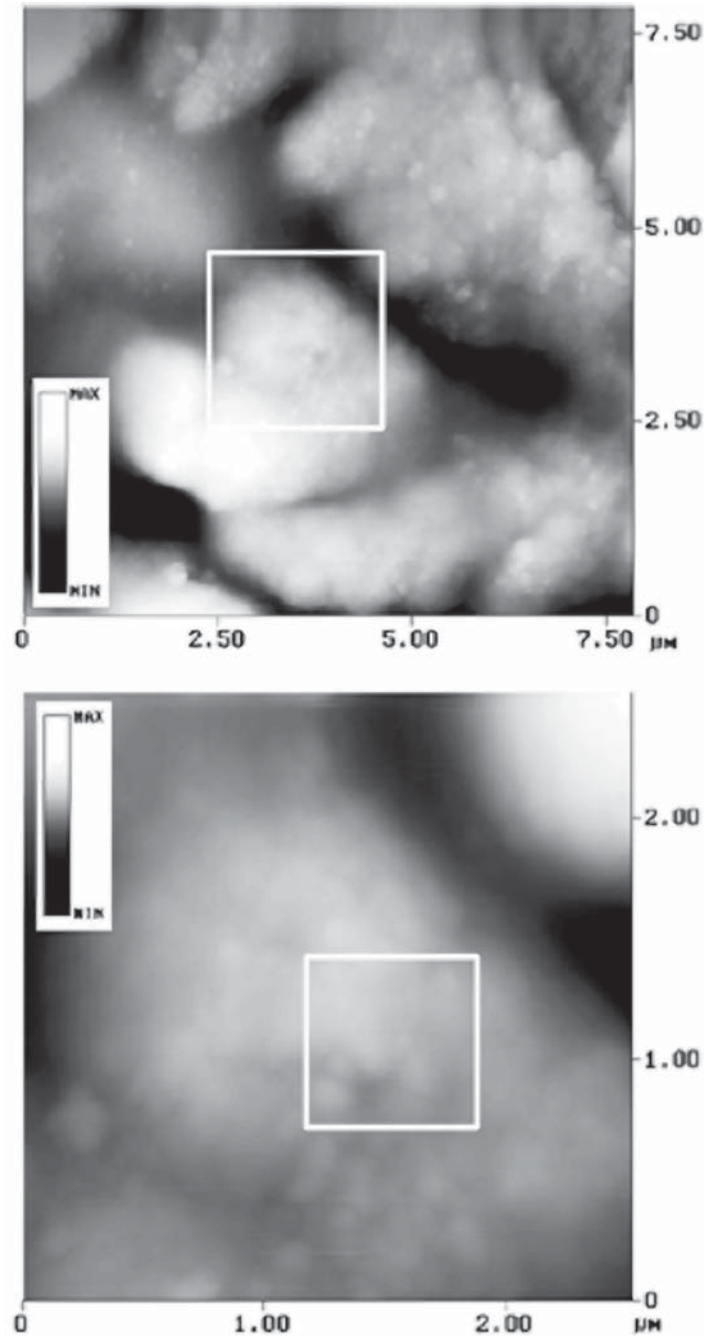

Fig. 3. Zooming in on chondrocyte topography. Frame marks zooming area of next image.

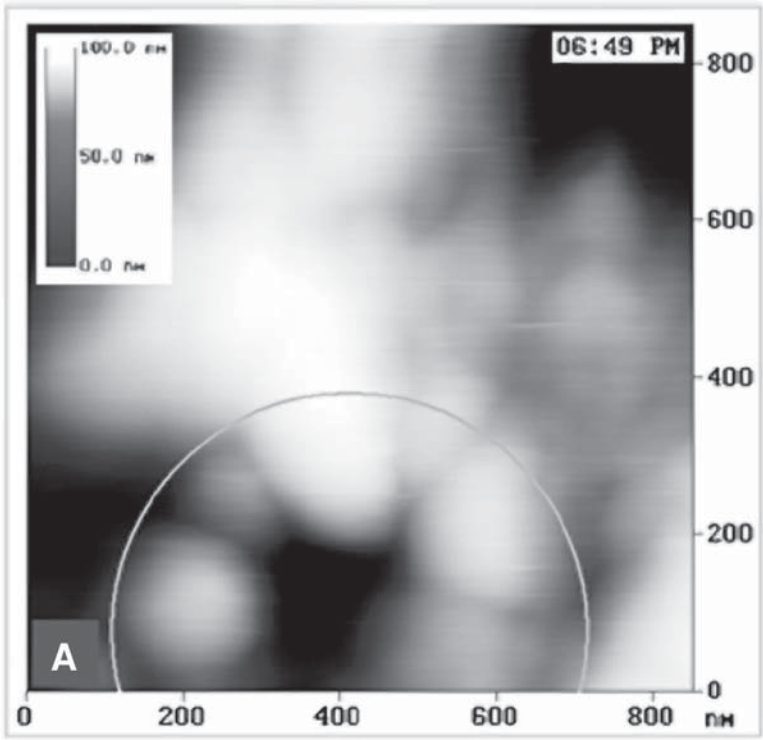

Fig. 4. Comparison between height and friction mode imaging. AFM observation of chondrocytes in buffer. The measurement time is shown in each picture. All images span an actual field of 850 × 850 nm. **(A)** Topography scan over 1 h simultaneous in height and friction mode. The approximate pore diameter is reduced from 382 ± 10 nm to 338 ± 10 nm.

tip, further investigation had to be done after replacing the tip. These effects and objections are described in more detail in **Subheading 5.**

7. Notes on Specific Details

7.1. Adherent Growing Cells Pose a Problem: Their Topography is Too Complexly Exhibited for Scanning

AFM was used to investigate different viable cells. Scanning whole cells under physiological conditions, in media or buffer solutions, poses some problems ***(12,16,18)***.

Since most cells are too large to observe them as a whole (**Fig. 5**), only portions of the cells can be investigated. **Figs. 7** and **8A** (pp. 117, 118) show rare examples of cancer cells that are small enough to scan whole. Numerous

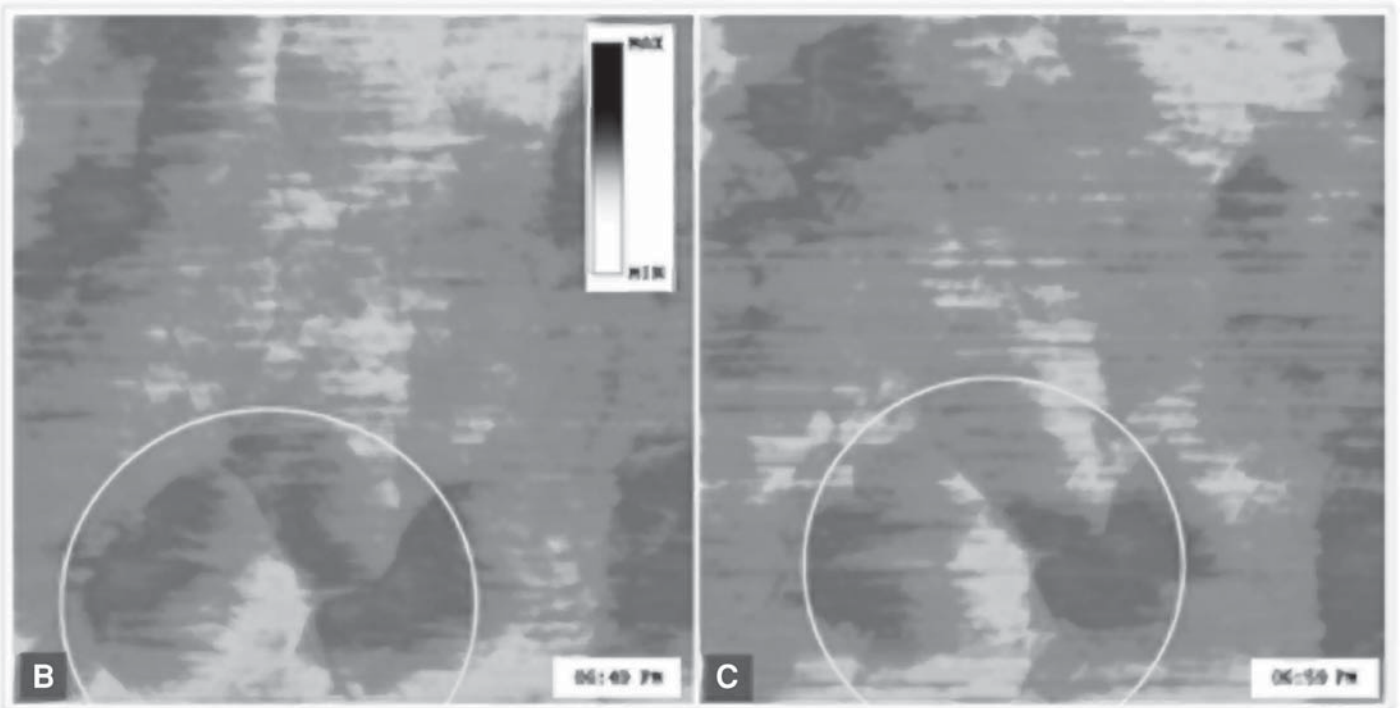

Fig. 4. **(B,C)** Large potential differences in the friction image of several measurements indicate an active part of the cell surface. During the pore diameter reduction, the surface potential in the immediate vicinity changes noticeably. A circle marks one active center on the cell surface. The timely changed contrast in friction mode between measurements indicates diminishing cell surface activity. This can be studied with much more detail by using different colors ***(15)***.

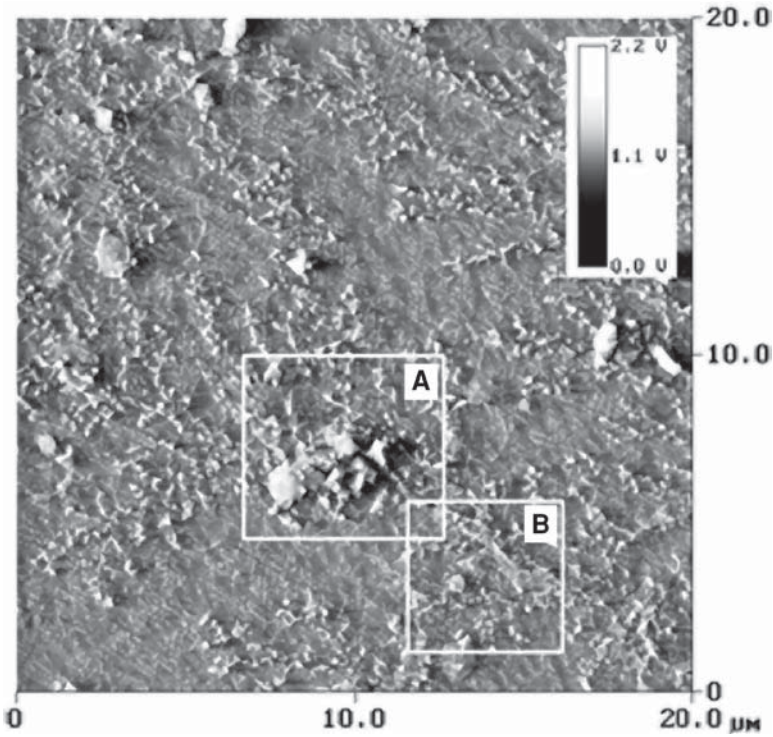

Fig. 5. Overview of the flat epithelial HOS cell in buffer observed in deflection mode. The secretion on the cell surface is monitored (some cell excrements in frame B are magnified in **Fig. 6**).

problems result in investigating the identical local position several times by AFM, after the material has left the Nanoscope instrument for other investigations. Molecular marker might help to solve this problem.

7.2. High Resolution Imaging of Cell Surfaces Requires Tight Attachment to Substrates

Imaging of loosely adhered cells enabled determination of the cell size and investigation of larger structures and pseudopodia but failed in resolving more detail.

7.3. Highly Dynamic Cell Surfaces Require Fast Scan Rates

Measurements in air only allow for limited examinations of the cells. Drying up processes strongly change the cell surface. As quickly as 10–30 min after beginning, dynamic interactions could no longer be monitored. Usually the cell structure collapses (example given in **Fig. 7**). When no dynamic

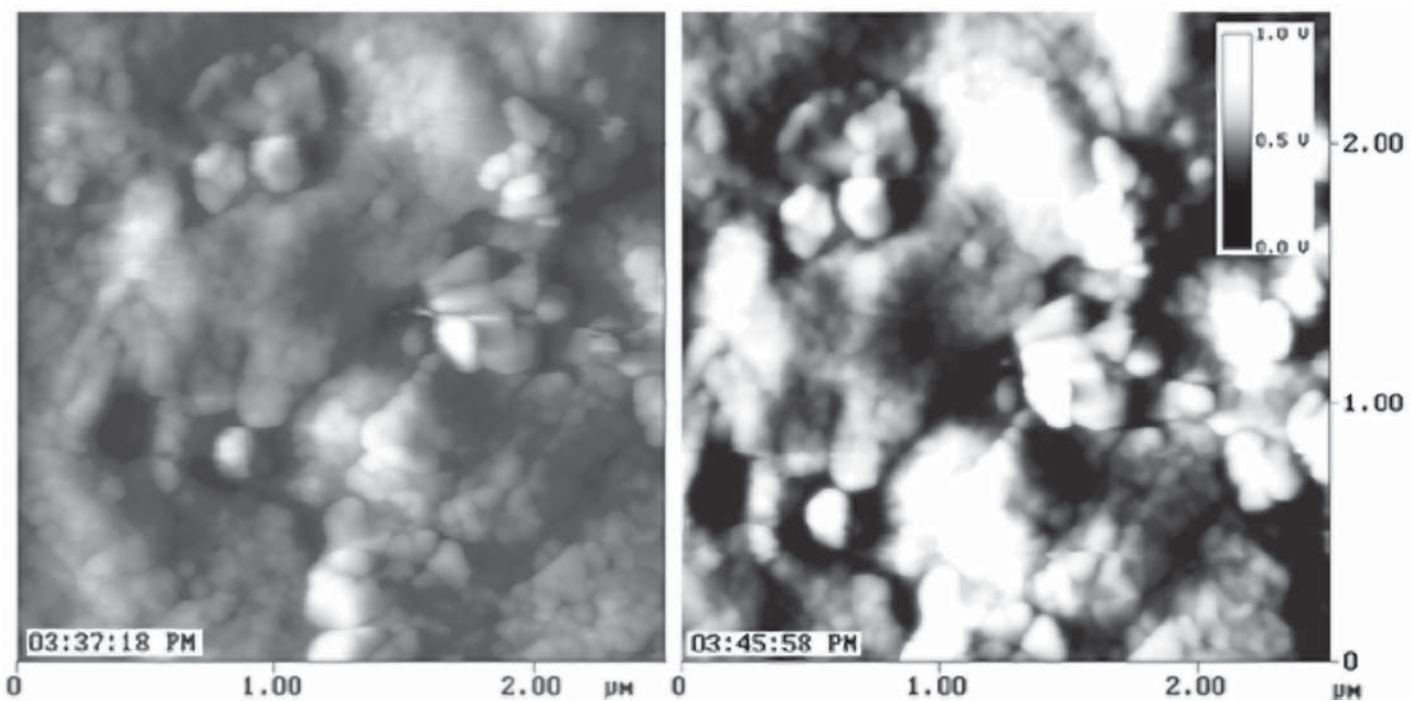

Fig. 6. Zooming in on frame B of **Fig. 5** (same z scale for both figures). Increasing contrast in the deflection mode indicates growing roughness of the surface.

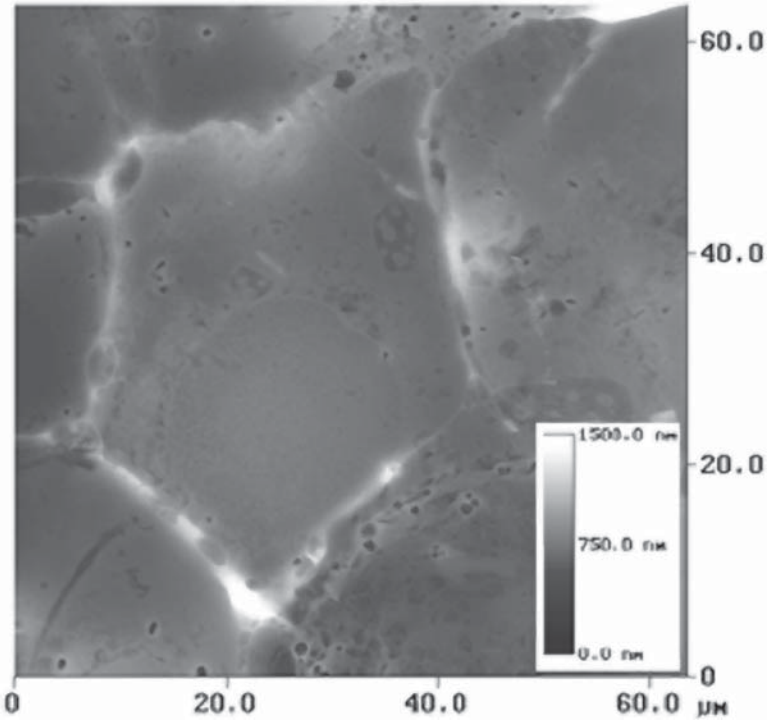

Fig. 7. Collapsed cell structure obtained in height mode AFM. The shape of the nucleus is visible. The cell margins (five white edges) are lifted on account of drying processes.

changes were detected (usually after 30 min), the scan rate can be reduced from 5–0.2 Hz to increase image quality and resolution.

Fast scan rates in buffer induce several troubles (such as buffer turbulences) and undefinable cell vibration. Therefore, the scan rate is critical and dynamic interactions can only be monitored with restriction.

7.4. The Buffer Sometimes Crystallizes During Liquid Evaporation

Under the required conditions, the buffer frequently crystallizes during liquid evaporation. These crystals can be identified easily by their symmetric structures (phosphate buffer crystals are marked out in **Fig. 8A**).

7.5. Protein Serum Covers the Cell Surface Like a Dense Carpet

The protein cover from a cell-culture procedure resembles to a high degree the protein surface of the washed cells, but it demonstrates a more homogeneous friction signal showing small changes with time. However, to distin-

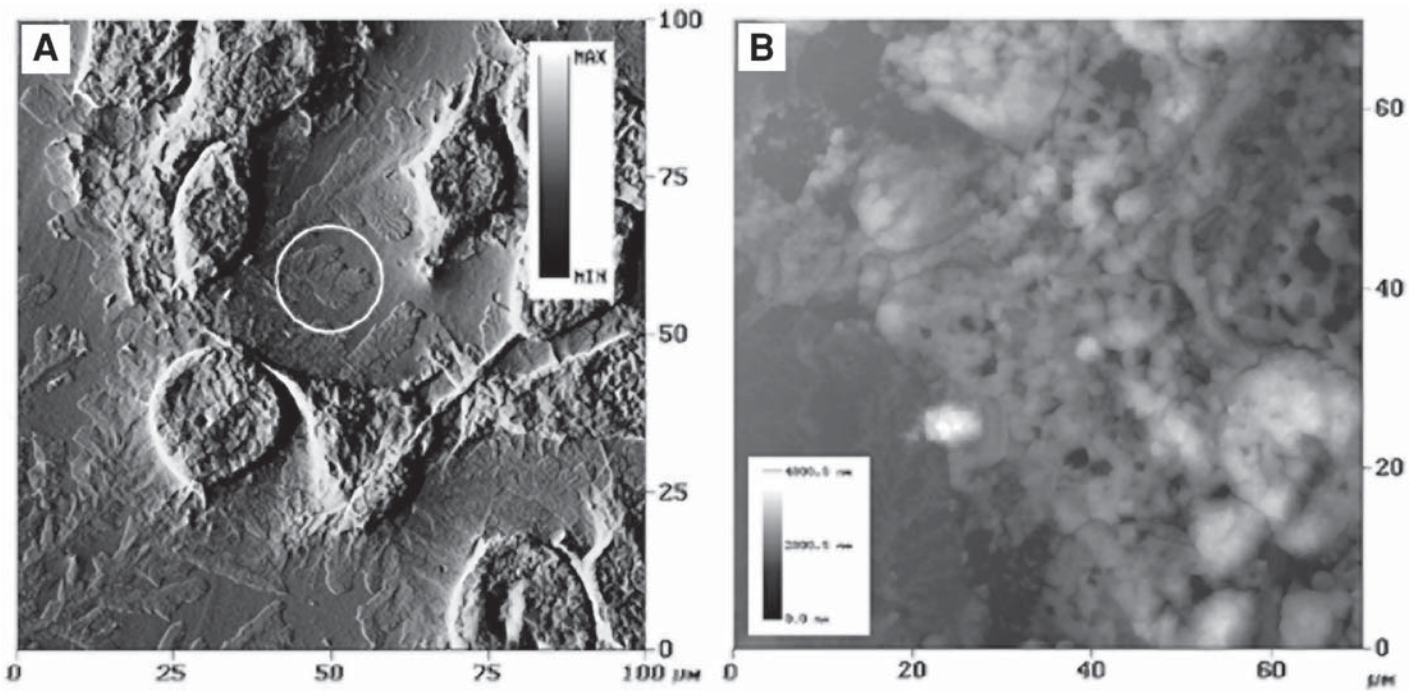

Fig. 8. Collection of frequent artifacts. **(A)** crystallization of phosphate buffer during liquid evaporation (*circle*); deflection mode data. **(B)** Serum protein layer from cell culture medium covers the cells (*see* **Subheading 7.5.**); height mode data.

guish between the serum cover and the actual cell surface is at times very difficult (*see* **Fig. 8B**). Rinsing the cover slips with PBS several times before AFM observation is always necessary to remove the coating.

7.6. Soft Collagen Material Differs Clearly from Viable Cell Material

As shown in the force calibration plots of pure collagen material (**Fig. 9**), the tip–surface interaction can be discriminated easily from active cell parts by the shape of the curve. Approaching the surface over a long range (around several micrometer) leads to a low-force indentation of the tip into the moist and soft collagen matrix (**Fig. 9A**). No change in the shape of the force curve can be observed by retracting the tip. Therefore, it can be concluded that the tip has no attraction or repulsion interaction with the collagen sample. This can be used as reference to identify local collagen collectives (*see* **Figs. 5** and **6**).

When collagen dries up, it becomes a stiffer material with less depth and consequently it would receive a shallower indentation. An example is shown in **Fig. 9B** and **C**. The sample structure collapses after water evaporation (*see* *x*-axis). As the sample is approached to the tip, a strong positive linear cantilever deflection is observed after contact when the tip and sample move toghether. When the motion of the sample is inverted (retracting portion of the curve), a similar cantilever deflection line is traced, but this time shifted several nanometers due to tip and sample remaining in contact.

7.7. The Shape of the AFM Tip Is Always Critical in Sample Measurements

The quality of the tip (e.g., radius of curvature, morphology, hardness, and surface composition) influences strongly the quality of AFM investigations. Most commercially available tips have a curvature radius of 30–50 nm with a pyramidal geometry. (Several others alter the tip morphology to enhance imaging capabilities.) Additionally, the tip may bind proteins or membrane debris that diminish the resolution. Special coatings exploit this situation and make molecular interaction force measurements possible ***(12)***.

7.8. Attraction and Repulsive Interactions of the Tip Cause Misinterpretations, Especially With Viable Cells

Typically, when the tip approaches the surface, the deflection value increases to the set point, indicating surface contact. As soon as the tip is in contact with the cell surface, the active cell induces electronic signals by disturbing the scan. Sometimes, it seems that the cells are tickled by the tip (or the applied potential) and shake themselves. This movement overestimates the determined cell-size (**Fig. 10**; **ref.** ***20***). Force-distance curves display uncontrolled vibrations of the tip. Undefinable surface tension forces could influence tip retraction (local attraction and repulsive forces could be detected).

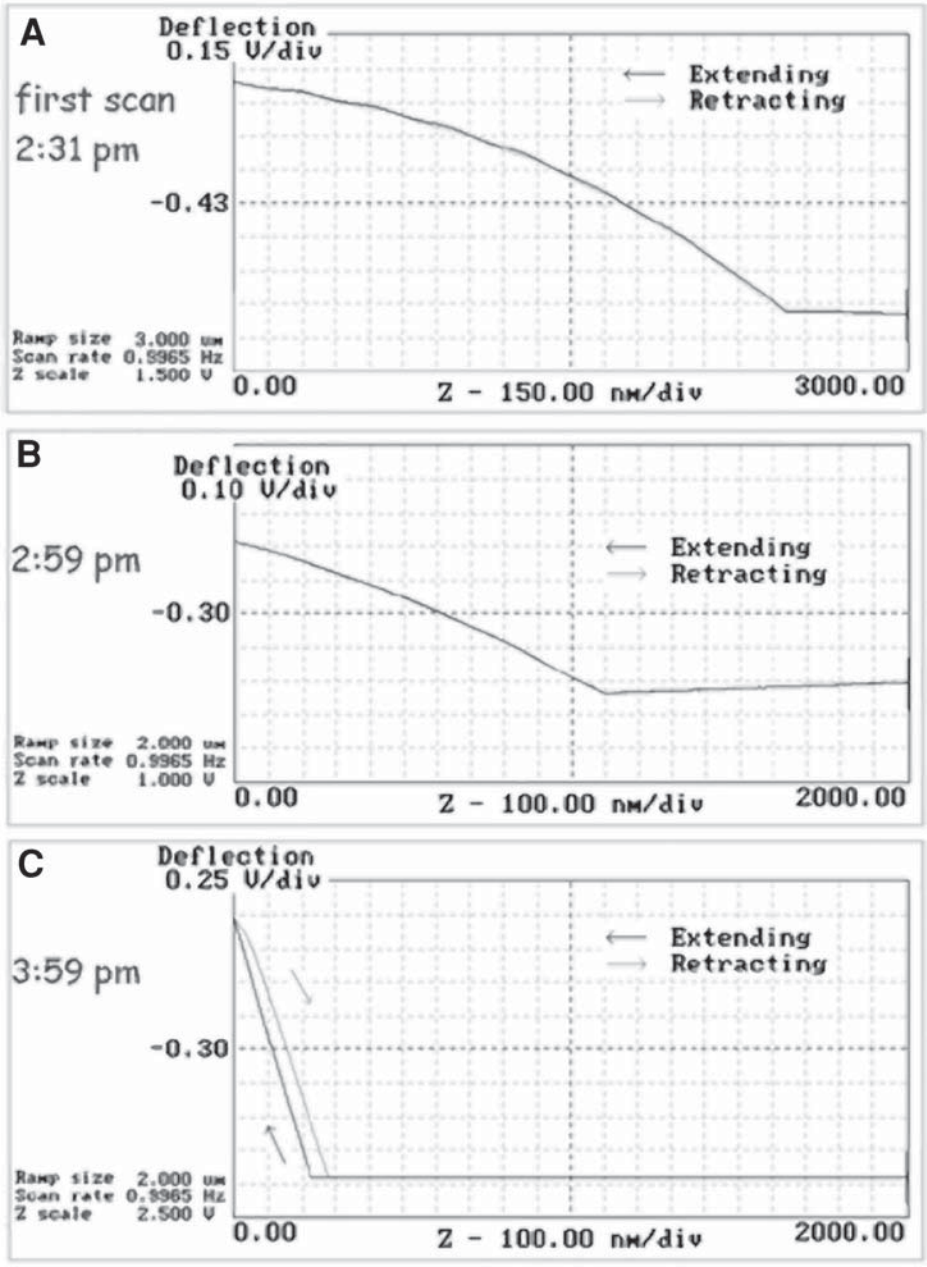

Fig. 9. Force calibration plots of dried up collagen material isolated from fibroblasts. The spring constant is 0.1 N/m. **(A)** Soft collagen sample with high amount of water. The average slope is about 0.4 mV/nm. **(B)** Partly dried up sample. The average slope is about 0.5 mV/nm. **(C)** Dry collagen sample. The average slope is about 6.0 mV/nm. Observation time is indicated.

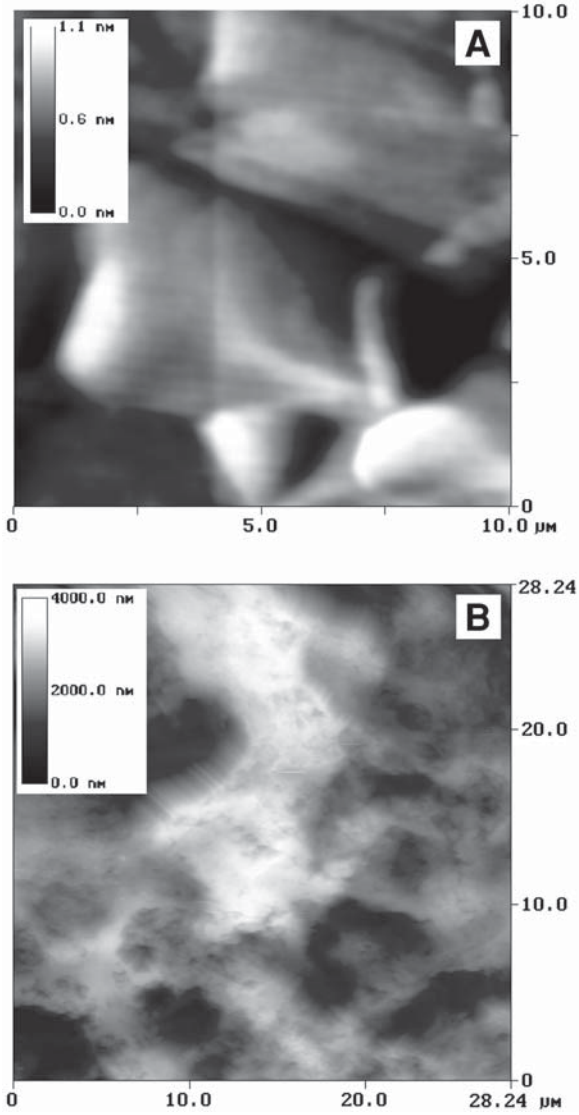

Fig. 10. AFM observation of adherently growing cells (hypopharynx carcinoma) ***(16)***. ***(A)*** Viable cells investigated in noncontact mode. The cells are displayed with an unreal softness. The *z* deflection changes by only a few nanometers. **(B)** Viable cells investigated in contact mode. Released from tip–surface contact the cells induce electronic signals and move. The *z* range changes are large. This movement overestimates the determined cell-size (same cell as **Fig. 10A**).

By repeating the approaching procedure to physical contact, nearby the set point (ΔU about –0.1 V) the tip–sample distance jumps to higher values and

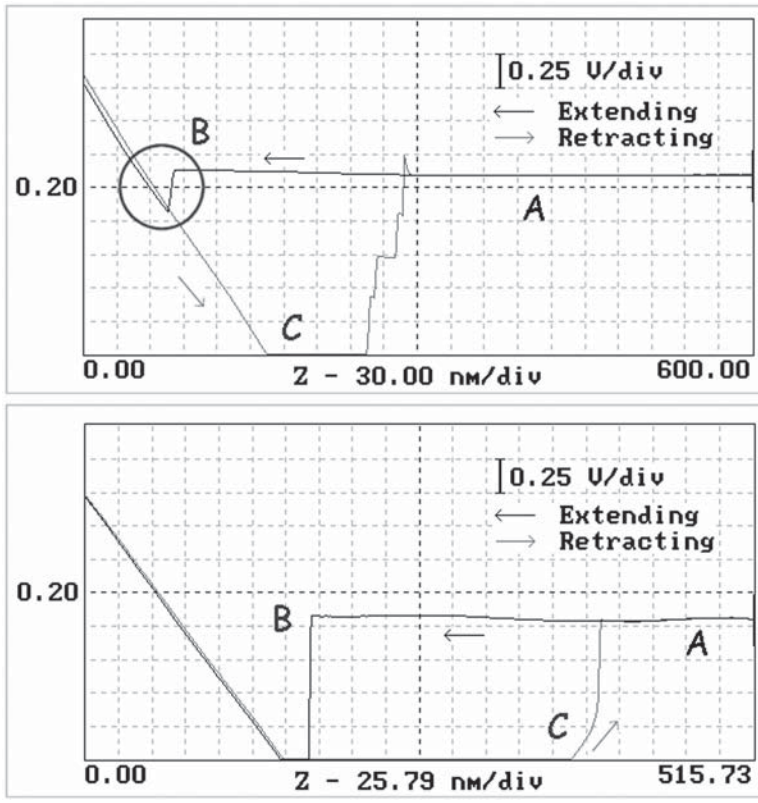

Fig. 11. Force–distance curve of a sample, which induce strong tip–sample interactions. Black line, approach curve; gray line, retraction curve. **(A)** At large tip–sample separations, there is no detectable interaction force. As the distance decreases, long- and short-range forces can be determined. **(B)** At some separation, the gradient of interaction energy exceeds the restoring force of the cantilever and the tip jumps to contact with the surface. If the interaction is too strong (bottom), no successful scan can be performed. **(C)** As the tip moves further in the negative z-direction (retracting), the restoring force exerted by the bending of the cantilever overcomes the adhesive force of the tip–sample contact and the tip breaks away from the sample. An idealized curve shows strong linear lines as shown in **Fig. 1**. The deflection curves presented here indicate tip contamination.

evades a successful approach. Strong tip vibrations are observed. An explanation could be that the cell dodges or repels the tip (data not shown). Even after a while, viable cells seem to remember the procedure, because they induce strong tip vibrations and make repeated scans impossible. Moving to another part of the sample (tested up to a few millimeters) cannot prevent the repul-

sion. If such a phenomenon occurs, another successful approach and further investigation are impracticable.

To avoid such troubles the force and the cantilever sensitivity have to be optimized. A higher spring constant prevents the uncontrolled vibration of the tip, but results more often in cell damage. When the interaction between the tip and the surface is very strong, it seems very much like a scan done in honey or highly viscous material. Tip contamination often occurs. This is explained in detail in **Fig. 11**.

7.9. Cells Can Contaminate or Stick to the Scanning Tip

Occasionally during the scanning procedure, the tip is covered with an indefinite cluster. Tip-biofouling caused by cellular damage and pick-up of loosely adhered particles generate artifacts that will compromise the experiment. Since the tip geometry is critical for force measurements and accurate topography determination, this has to be avoided in all cases.

Acknowledgments

The illustrations presented would not have been made without the encouragement and cooperation of Grit Helbing, Ottilie Pietz, and Angela Rosemeier of the Medical Faculty Halle. Their help is gratefully acknowledged. The authors thank Robert Bischoff and SENSOBI Sensoren GmbH. Their instrumental service is highly appreciated. The Ministry of Culture and Education of Saxony–Anhalt and the BMBF have supported our research.

References

1. Ricci, D. and Grattarola, M. (1994) Scanning force microscopy on live cultured cells: imaging and force-versus-distance investigations. *J. Microscopy* **176,** 254–261.
2. Oberleithner, H., Brinckmann, E., Giebisch, G., and Geibel, J. (1995) Visualizing life on biomembranes by atomic force microscopy. *Kidney Int.* **48,** 923–929.
3. Wohlrab, D., Wohlrab, J., Reichel, H., and Hein, W. (2001) Is the proliferation of human chondrocytes regulated by ionic channels? *J. Orthop. Sci.* **6,** 155–159.
4. Grodzinsky, A. J., Levenston, M. E., Jin, M., and Frank, E. H. (2000) Cartilage tissue remodeling in response to mechanical forces. *Annu. Rev. Biomed. Eng.* **2,** 691–713.
5. Hein, H.-J., Brandt, J., Bernstein, A., Engler, T., and Weisser, L. (1997) Zur Darstellung der Mikrostruktur des Knochens mit dem Raster-Sondenmikroskop. *Z. Med. Phys.* **7,** 21–26.
6. Henning, S., Adhikari, R., Michler, G. H., Seidel, P., Sandner, B., Bernstein, A., and Hein, H.-J. (2001) Analysis of the bone-implant interface of a partially resorbable bone cement by scanning electron and scanning force microscopy, in *Micro- and Nanostructures of Biological Systems*, (Bischoff, G. and Hein, H.-J., eds.), Shaker-Publ., Aachen, pp. 109–120.

7. Oda, Y., Matsumoto, Y., Harimaya, K., Iwamoto, Y., and Tsuneyoshi, M. (2000) Establishment of new multidrug-resistant human osteosarcoma cell lines. *Oncol-Rep.* **7,** 859–866.
8. Rodan, S. B., Imai, Y., Thiede, M. A., Wesolowski, G., Thompson, D., Bar-Shavit, Z., et al. (1987) Characterization of a human osteosarcoma cell line (Saos-2) with osteoblastic properties. *Cancer Res.* **47,** 4961–4966.
9. Rhim, J. S. (1993) Neoplastic transformation of human cells in vitro. *Crit. Rev. Oncogene* **4,** 313–335.
10. Sakai, K., Mohtai, M., and Iwamoto, Y. (1998) Fluid shear stress increases transforming growth factor beta 1 expression in human osteoblast-like cells: modulation by cation channel blockades. *Calcif. Tissue Int.* **63,** 515–520.
11. Grimsehl, E., (1989) *Lehrbuch der Physik Vol. 1: Mechanik, Akustik, Wärmelehre*, 25th ed. Teubners-Verlagsgesellschaft, Leipzig. pp. 43–56.
12. Takano, H., Kenseth, J. R., Wong, S.-S., O'Brien, J. C., and Porter, M. D. (1999) Chemical and biochemical analysis using scanning force microscopy. *Chem. Rev.* **99,** 2845–2890.
13. Hansma, H. G. (2001) Surface biology of DNA by atomic force microscopy. *Annu. Rev. Phys. Chem.* **52,** 71–92.
14. Linder, A., Weiland, U., and Apell, H. J. (1999)Novel polymer substrates for SFM investigations of living cells, biological membranes, and proteins. *J. Struct. Biol.* **126,** 16–26.
15. Bischoff, R., Berghaus, A., and Hein, H.-J. (1997) Inspection of silicone-biomaterials using SPM. *Biomed. Techn.* **42(Suppl. 2),** 482–483.
16. Bustamante, C. and Keller D (1995) Scanning force microscopy in biology. *Physics Today* 32–38.
17. Benoit, M., Holstein, T., and Gaub, H. E. (1997) Lateral forces in AFM imaging and immobilization of cells and organelles. *Eur. Biophys. J.* **26,** 283–290.
18. Bischoff, G. and Langner, J. (2001) SFM of living cells—a study of the method, in *Micro- and Nanostructures of Biological Systems*, (Bischoff, G. and Hein, H.-J., eds), Shaker Publ., Aachen, pp. 135–152.
19. Bischoff, R., Bischoff, G., and Hein, H.-J. (2002) Scanning force microscopy (SFM) visualization of adherently growing cells. *Am. Biotech. Lab.* **3,** 20–22.
20. Bischoff, R., Bischoff, G., and Hoffmann, S. (2001) Scanning force microscopy observation of tumor cells treated with hematoporphyrin IX derivatives. *Ann. Biomed. Eng.* **29,** 1092–1099.